Systematics of continuum angular distributions: Extensions to higher energies

C. Kalbach
Physics Department, Duke University, Durham, North Carolina 27706
(Received 21 December 1987)

The systematics of continuum angular distributions in nucleon- and alpha-particle-induced reactions at energies up to several hundred MeV have been studied and parametrized. It has been confirmed that at lower bombarding energies the shapes of the angular distributions are determined mainly by the kinetic energy in the exit channel, and by the division of the cross section into its multistep direct and multistep compound parts. For incident nucleons with energies above 130 MeV there is a change in the systematics, and the ratio of the energies in the exit and entrance channels of the reaction becomes the important energy parameter. Small second order dependences are also evident for nucleon-induced reactions. The systematics are parametrized using exponentials in $\cos\theta$ and a small number of universal parameters.

I. INTRODUCTION

The present work represents an effort to extend earlier results on the systematics of continuum angular distributions to higher energies, to improve the systematics at low emission energies, and to look for second order dependencies of the angular distributions on various reaction parameters.

A. The Kalbach-Mann systematics

The year 1981 saw the publication of what have since become known as the Kalbach-Mann systematics[1,2] for continuum angular distributions in light particle nuclear reactions. These systematics describe the shapes of the angular distributions for inclusive reactions at incident energies up to 80 MeV and emission energies up to 60 MeV.

In the Kalbach-Mann (KM) systematics, the angular dependence of the inclusive cross section was found, at least to first order, to be independent of the bombarding energy and the nature of the projectile, target, and emitted particle. Rather, it is determined primarily by the energy of the emitted particle and the fraction of the time that it was emitted in a multistep direct (MSD) process rather than a multistep compound (MSC) one. The observed systematics were parametrized in terms of Legendre polynomials using only a small number of universal parameters.

While the KM systematics have been quite successful at reproducing data in a wide variety of applications over the intervening years, they have problems at both high and very low emission energies. At high emission energies the MSD angular distributions become strongly forward peaked, and it becomes increasingly difficult to reproduce the smooth behavior of the data at back angles using Legendre polynomials. At the other end of the scale, the systematics do not predict isotropy of the angular distributions as the emission energy goes to zero.

One additional disadvantage of the KM systematics is that second order dependencies on other reaction parameters could not be studied. The information on such dependencies is spread among up to six reduced Legendre coefficients and thus is difficult to discern.

In spite of these difficulties, the KM systematics continue to play an important role in preequilibrium reaction studies. One reason is that the literature still displays a variety of angular distribution models which make differing assumptions. Second, no other approach is applicable to as wide a variety of reactions and is as simple to use as the KM results. Finally, there is still no explanation of the observed similarity of the angular distributions in reactions with varying projectiles and emitted particles.

B. Other approaches

The generalized exciton model[3,4] (GEM) has gained acceptance as a somewhat realistic but still nonmicroscopic approach to preequilibrium angular distributions. This concensus is, however, somewhat offset by the diversity of modifications to the model which have been proposed.

To better reproduce experimental angular distributions for (nucleon-nucleon) reactions at backward angles, additional physics has been introduced, destroying much of the simplicity of the exciton model. Various groups have tried the following improvements in various combinations: (a) replacing free nucleon-nucleon scattering information with nuclear matter results (including Pauli principle and Fermi motion effects) based either on a Fermi gas[5–7] or a harmonic oscillator[8] model, (b) considering refraction effects,[6,9] (c) including angle-energy correlations,[6–8] (d) including the effects of the finite nucleon temperature,[9] and (e) using the GEM only for the MSD part of the preequilibrium cross section, with the MSC part assumed to be isotropic.[10]

Two other difficulties with the GEM are that it is not readily applicable to reactions involving complex particles, and that, like the KM systematics, it uses Legendre polynomials so that it cannot be used at emission energies above 50 to 60 MeV.

While the GEM is certainly an interesting and promis-

ing avenue to pursue, these difficulties certainly leave room for a more phenomenological approach to be investigated as well.

A similar approach has been employed in the geometry dependent hybrid model,[11] and in that connection Blann *et al.* have raised a number of concerns about all such semiclassical methods.

Quantum mechanical methods[12,13] are also used, but their calculations are far too time consuming for large scale applications, and again differing assumptions are made.

C. The present work

The present work represents an effort to remove the difficulties in the Kalbach-Mann systematics and to extend them to bombarding energies of several hundred MeV. Section II of this paper gives a brief review of the Kalbach-Mann systematics, while Sec. III discusses the method used to study the systematics of the data. Section IV considers the possible origin of extra apparent cross section sometimes seen at forward angles, Sec. V gives the observed systematics, and Sec. VI describes their parametrization. Calculated angular distributions are compared with the data in Sec. VII. A more complete description of this work can be found in Ref. 14.

II. REVIEW OF THE KALBACH-MANN SYSTEMATICS

Mathematically, the angular distributions in the Kalbach-Mann systematics are described in terms of Legendre polynomials up through order 6. All of the polynomials contribute to the multistep direct component while only even order polynomials are used for multistep compound processes. It is assumed that the angle integrated, energy differential cross section and the fraction of it which is multistep direct are known from preequilibrium calculations[15] or from experiment. (At a large evaporation peak the cross section is nearly pure MSC while at the high energy end of a spectrum it is nearly pure MSD.)

The original work[1] used the total kinetic energy, ϵ_b, in the exit channel as the pertinent energy parameter, but later work[2] showed a preference for the parameter $e_b=\epsilon_b+B_b$ over either ϵ_b itself or $\epsilon_b+B_b-B_a$. Here B_b is the empirical binding energy of the emitted particle in the composite nucleus and B_a is the projectile binding energy. The reduced polynomial coefficients and, indeed, the calculated angular distributions are independent of the target, the projectile, and the emitted particle for all light particle induced reactions (except in so far as the nuclei involved determine the binding energies).

The high energy limit of these systematics occurs at emission energies around 50 MeV. The experimental cross section drops by more than 2 orders of magnitude between 0° and 180°, and the Legendre polynomials (which fluctuate between $+1$ and -1) can no longer cancel out at back angles to yield a smooth curve. Furthermore, the equations for the reduced coefficients imply that an infinite number of polynomials would be needed at energies of 90 or 100 MeV.

At very low emission energies, the parametrization does not produce isotropy at either $\epsilon_b=0$ or at $e_b=0$ ($\epsilon_b=-B_b$, corresponding to zero energy above the Fermi level of the emitting nucleus). At $e_b=0$, the largest reduced coefficients are b_1 and b_2 which are 10% and 1%, respectively, of their asymptotic values. Since the cross section is expected to be nearly pure MSC, the value of b_1 is not important and the deviations from isotropy should be very small. Still, some users of the systematics have felt it necessary to modify them to correct this low energy behavior.

III. THE METHOD

The necessary ingredients for improving the KM systematics and extending them to higher energies are a broader data base, a mathematical form to replace the Legendre polynomials, and a requirement of reasonable behavior at very low emission energies.

A. The data base

The data used in the present study includes nearly all of the nucleon- and alpha- particle-induced angular distributions used in the original work.[1] These were supplemented with a large number of angular distributions from reactions at higher bombarding energies and additional data at the lower energies. The data systems[16–39] are listed in Tables I–III, and are all for inclusive reactions. The targets range from ^{12}C to ^{232}Th, and all emitted particles with mass numbers up to four were considered. The bombarding energies extend up to 720 MeV, although both the quality and quantity of the data prohibit the fitting of the parametrization above about 200 MeV.

Most of the data are given in the laboratory frame of reference, and it was necessary to transform them into the center of mass. For the higher energy systems this transformation was done relativistically. It was assumed that all of the particles were emitted from the original composite nucleus. This, of course, will not always be the case, but even for the very light targets, there are only a few instances where the assumption causes any obvious problems. In these cases a slight apparent rise is noted in the cross section at back angles above the straight line trend of the more forward angle data. Otherwise the assumption of emission from the original composite nucleus seems adequate.

Another common difficulty with continuum reaction data is the presence of experimental background, particularly at very forward angles where additional components may also contribute. The differentiation between these two situations is discussed in Sec. IV.

B. The assumed angular dependence

The most obvious angular dependence to replace the Legendre polynomials for describing the MSD cross sections is an exponential decay with angle. Here an exponential in $\cos\theta$ was chosen since it yields a smooth turnover of the cross section at 0° and 180° and since $d\Omega=d\cos\theta\, d\phi$. It was then verified that calculated angular distributions for pure MSD reactions based on the

TABLE I. Data for inclusive neutron induced reactions.

Reaction	Target	Proj. energy (MeV)	Channel energies Range (MeV)	No.	No. fit	Lab. angles Range (deg)	No.	Ref.
(n,n')	Fe-Bi	26	16–23.5	17	8	25–140	7	16
(n,p)	Nb	14	7–11	3	1	24–164	16	17
(n,p)	Ni	60	21.5–52.4	13	13	6–70	12	18
(n,α)	Nb	14	11–17	4	2	24–164	16	19
(n,α)	Nb	15	11–17	4		45–140	3	20
Total				41	24			

TABLE II. Upper: data for inclusive (p,nucleon) reactions. Lower: data for inclusive (p,complex) reactions.

Reaction	Target	Proj. energy (MeV)	Channel energies Range (MeV)	No.	No. fit	Lab. angles Range (deg)	No.	Ref.
(p,n)	Rh,Ag	18	5.5–12.5	8	2	4–144	10	21
(p,n)	Ag	25	6.5–18.5	5		4–159	16	22
(p,n)	Al-Zr	90	20–75	32	32	30–135	6–7	23
(p,n)	Al-Pb	590	120–400	25	10	30–150	3	24
(p,p')	Fe,Au	29	4–20	6	2	30–125	4	25
(p,p')	Fe,Bi	39	5–30	11	6	15–120	4–7	25
(p,p')	C-Bi	62	4–55	37	23	12–160	5–18	25
(p,p')	Al-Bi	90	15–80	46	45	20–140	6–9	26
(p,p')	Ni	100	15–90	16	16	25–155	8	26
(p,p')	Al-Pb	165	35–140	30	29	25–150	6–12	27
(p,p')	Al,Au	200	10–180	25	24	14–135	5	28
(p,p')	Al-Bi	450	130–360	22		30–60	3	29
(p,p')	Fe,W	558	60–460	35	35	10–60	6	30
(p,p')	Al,Ta	600	120–360	15	14	30–150	5	31
	Total ($E_{inc} < 300$ MeV)			228	191			
	Total ($E_{inc} > 300$ MeV)			97	59			
(p,d)	Fe	29	4,7	2		15–125	5	25
(p,d)	Fe,Bi	39	7–25	7	3	15–120	4–7	25
(p,d)	Fe,Sn	62	5–42	17	9	12–160	20–21	25
(p,d)	Al-Bi	90	25–80	44	44	20–140	9	26
(p,d)	Ni	100	30–75	6	6	15–155	9	26
(p,d)	Ni	165	40–140	11	11	25–150	12	27
(p,d)	Al,Au	200	30–140	23	23	14–135	5	28
(p,d)	Al-W	558	100–360	43	43	10–60	6	30
(p,t)	Fe,Bi	39	10–30	7	2	12–120	4–7	25
(p,t)	Fe,Sn	62	10–42	14	6	12–160	20–21	25
(p,t)	Al-Bi	90	15–80	31	31	20–140	9	26
(p,t)	Al,Au	200	30–110	17	17	14–135	5	28
(p,^{3}He)	Fe	62	24–33	6	4	12–160	21	25
(p,^{3}He)	Al,Bi	90	25–75	9	9	20–140	9	26
(p,^{3}He)	Al,Au	200	30–90	12	12	14–135	5	28
(p,α)	Fe,Au	29	8–22	5		15–130	4–5	25
(p,α)	Fe,Bi	39	8–40	10	1	15–120	4–7	25
(p,α)	C-Bi	62	10–55	24	9	12–160	6–21	25
(p,α)	Al-Bi	90	30–80	29	29	20–140	9	26
(p,α)	Ni	165	40–150	7	7	25–150	13	27
(p,α)	Al,Au	200	40–100	13	13	14–135	5	28
	Total ($E_{inc} < 300$ MeV)			294	296			

TABLE III. Data for inclusive alpha-particle-induced reactions.

Reaction	Target	Proj. energy (MeV)	Channel energies Range (MeV)	No.	No. fit	Lab. angles Range (deg)	No.	Ref.
(α,p)	Ni	36	4–25	3		20–150	8	32
(α,p)	Co,Rh	42	10–32	10	6	10–159	10–11	33
(α,p)	C,Fe	59	6–40	11	4	20–120	5–6	34
(α,p)	Al,Ni	100	25–75	21	21	20–150	7–8	35,36
(α,p)	Al-Th	140	15–100	33	33	20–140	8–11	37
(α,p)	Ni	172	30–80	6	6	20–155	8	36
(α,p)	Al,Ta	720	70–190	19	19	30–150	5	38
(α,d)	Ni	36	5–19	3		20–150	8	32
(α,d)	Fe	59	6–33	8	5	20–122	6	34
(α,t)	Ni	36	6–18	3		20–150	8	32
(α,t)	Fe	59	8–31	5	2	20–122	6	34
(α,α′)	Ni	36	10–28	3		30–150	7	32
(α,α′)	C,Fe	59	7–45	11	6	20–122	5–6	34
(α,α′)	Fe	90	36–66	4	4	15–140	10	39
(α,α′)	Mg,Al	100	30–80	8	8	20–113	7	35
(α,α′)	Fe	120	33–103	8	8	10–160	11	39
(α,α′)	Al-Th	140	20–110	46	42	20–120	7–11	37
(α,α′)	Fe	160	70–140	8	8	15–105	6	39
	Total ($E_{\text{inc}} < 300$ MeV)			191	153			
	Total ($E_{\text{inc}} > 300$ MeV)			19	19			

KM systematics follow this dependence with extreme accuracy for emission energies below 40 MeV (where back angle bumps begin to appear).

The mathematical form for the MSD part of the angular distributions is determined by requiring that angle integration yield the correct energy differential cross section, $d\sigma_{\text{MSD}}/d\epsilon_b$. The result is

$$\frac{d^2\sigma_{\text{MSD}}}{d\Omega\, d\epsilon_b} = \frac{1}{4\pi}\frac{d\sigma_{\text{MSD}}}{d\epsilon_b}\frac{2a}{e^a - e^{-a}}\exp(a\cos\theta)\ , \quad (1)$$

where θ is the emission angle in the center of mass frame. Based on the KM systematics, the slope, a, of the exponential for incident energies below 80 MeV should, to first order, be a function only of the energy parameter $e_b = \epsilon_b + B_b$.

The form for the multistep compound part of the angular distributions was assumed to contain exponentials with both positive and negative slopes, each having the same slope parameter, $a(e_b)$, as is used for the MSD part. This yields distributions which are symmetric about 90° in the center of mass and does not introduce any new parameters. Thus the MSC part of the cross section is given by

$$\frac{d^2\sigma_{\text{MSC}}}{d\Omega d\epsilon_b} = \frac{1}{4\pi}\frac{d\sigma_{\text{MSC}}}{d\epsilon_b}\frac{a}{e^a - e^{-a}}[\exp(a\cos\theta) + \exp(-a\cos\theta)]\ . \quad (2)$$

The resulting MSC angular distributions nearly coincide with the corresponding curves from the KM systematics when $a(e_b)$ is chosen to make the MSD angular distributions coincide.

Combining Eqs. (1) and (2) and expressing the exponentials as hyperbolic functions gives the general expression

$$\frac{d^2\sigma}{d\Omega\, d\epsilon_b} = \frac{1}{4\pi}\frac{d\sigma}{d\epsilon_b}\frac{a}{\sinh(a)}[\cosh(a\cos\theta) + f_{\text{MSD}}\sinh(a\cos\theta)]\ . \quad (3)$$

Once again, the angle integrated cross section $d\sigma/d\epsilon_b$ and the fraction, f_{MSD}, of the cross section which is multistep direct are assumed to be known either from preequilibrium model calculations or from experiment.

Guaranteeing reasonable behavior for the angular distributions in the new systematics at very low emission energies is simply a matter of constraining $a(e_b)$ in this domain. This question is discussed in Sec. VI.

C. Analysis of the data

Most of the data in Tables I, II, and III for which the cross section was thought to be pure multistep direct were analyzed by plotting the double differential cross sections for a given emission energy as a function of $\cos\theta$ on semilogarithmic graph paper. For systems used in Ref. 1 the quantity f_{MSD} was taken from that work. At

higher bombarding energies, particles emitted at energies of at least 25 MeV were assumed to be from purely multistep direct processes, as they were at the lower incident energies. This assumption was later verified by observing that the data points followed the expected decay with $\cos\theta$.

In each case, a straight line was fit by eye through the data points, and a value for the slope $a(e_b)$ was extracted. These slopes were then studied to determine the systematics of the full ensemble of data. Since the object of the study was to determine general trends rather than precise slopes for particular angular distributions, the use of least-squares fitting was not deemed necessary. The tables indicate the number of angular distributions for each reaction which were actually fit to determine slope values.

IV. EXTRA FORWARD ANGLE CROSS SECTION

For many of the experimental angular distributions, the cross section at one or more of the most forward angles was clearly well above the trend set by the rest of the data points. In such cases the straight line fit was carried out ignoring these forward angle data. Unfortunately it is often not clear whether the extra cross section represents uncorrected background counts or an additional reaction mechanism. The mechanisms which are thought to be included in the main angular distribution systematics are (based on the work of Refs. 1 and 40) equilibrium evaporation, simple preequilibrium emission (both MSD and MSC), pickup and stripping reactions, and knockout and inelastic processes involving cluster degrees of freedom.

Background subtraction is a particularly difficult problem for continuum energy spectra and is generally most severe at very forward angles. In the absence of duplicate data from different laboratories, the problem of differentiating forward angle background from real data is partly a matter of conjecture and partly a matter of looking for systematic trends in the "extra" cross section.

A. Nucleon-induced reactions

For (p,p') reactions at energies up to 100 MeV, data taken using passive detector collimators show background due to slit edge penetration, primarily by elastically scattered particles.[41,42] Above 100 MeV, quasifree scattering becomes increasingly important, so energy-angle combinations with obvious QFS contributions have been eliminated from consideration.

The 18 and 25 MeV (p,n) data of Grimes *et al.*[21,22] are known to have forward angle background due to the tuning of the beam upstream of the target. This is likely also to be the origin of the extra cross section in the 90 MeV (p,n) data of Kalend *et al.*[23]

In general, the angular distributions get progressively cleaner as one goes from (p,p') and (p,n) to (p,d), (p,t), (p,^{3}He), and (p,α) reactions, and any observed extra cross section occurs only at the higher emission energies. Its origin is not known.

B. Alpha-particle-induced reactions

The extra forward angle "components" in the alpha-particle-induced reactions studied generally extend to larger angles than for their proton projectile counterparts and represent a larger fraction of the angle integrated cross section. Because they merge more gradually with the main component, they were not obvious in the work leading to the KM systematics but are clear in the $\cos\theta$ plots used in the present study. They are believed to represent real cross section and are discussed in more detail in Sec. VII C.

V. OBSERVED SYSTEMATICS

A. General trends

Plots were constructed of the slope values a versus the energy parameter $e_b=\epsilon_b+B_b$ for each combination of projectile and emitted particle. Each plot therefore

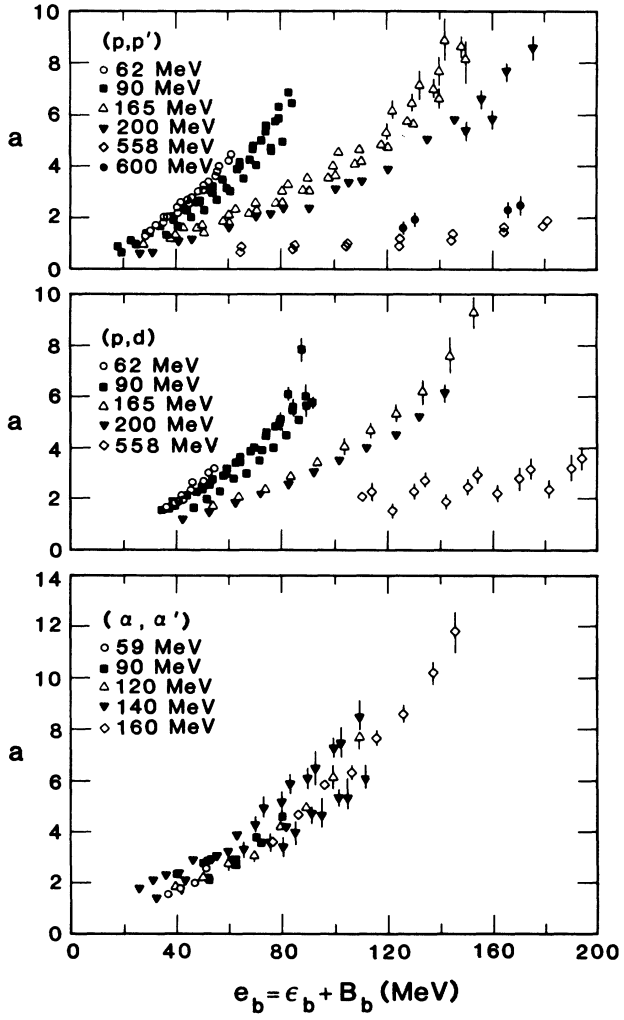

FIG. 1. Empirical slopes resulting from fitting experimental angular distributions with an exponential in $\cos\theta$ plotted vs the exit channel energy parameter e_b for several projectile-emitted particle combinations. The points are identified by their bombarding energies.

spanned a variety of targets and incident energies. A few of these plots for bombarding energies above 50 MeV are shown in Fig. 1.

For incident alpha particles, the points all cluster about a single curve as expected from the KM systematics. For incident protons the same seems to be generally true for bombarding energies up to 100 MeV. In addition, the general trend of the data points is the same for each projectile-emitted particle combination. Thus for incident proton energies up to around 100 MeV, and for incident alpha particle energies up to 160 MeV, the angular distributions are determined primarily by the emission energy, with at most a secondary dependence on target mass, bombarding energy, and type of emitted particle.

Data taken with 165–600 MeV protons, on the other hand, show slope values which fall ever further below those expected from the trends of the lower energy data. Figure 2 shows the (p,p′) results of Fig. 1 plotted versus e_b/e_a where $e_a=\epsilon_a+B_a$ is the entrance channel equivalent of e_b. The 165 and 200 MeV data now follow a single trend, and the 558 and 600 MeV data are brought into somewhat closer agreement with them. Whether the remaining differences are real or are simply due to the fragmentary nature of the 558 and 600 MeV data cannot be determined until more complete experimental work has been done.

In any event, it seems clear that there is a change in the physical parameter determining the shape of the angular distributions at incident proton energies somewhere between 100 and 165 MeV. A good candidate for the new parameter is the ratio e_b/e_a. The angular distributions are, however, still largely independent of target or emitted particle.

If a similar transition occurs for incident alpha particles, it must do so at incident energies above 160 MeV. The only data available which might show such an effect are the 720 MeV (α,p) results of Cordell *et al.*[38] However, while the slopes of these angular distributions are quite small (indicating that a transition may have occurred), the values from the two different targets do not agree with one another, and their behavior looks quite different from that observed for any of the other data systems. Thus, much more experimental work at intermediate bombarding energies is needed to be able to address this question adequately.

B. The choice of energy parameters

Because of the scatter in the slope values evident in Figs. 1 and 2, it is worth investigating the optimum energy parameters before proceeding to a parametrization. Here the 90 MeV proton data[26] were used.

The parameter ϵ_b was considered but (as found in Ref. 2) it did slightly worse than e_b, so a variant of e_b was considered.

The quantity e_b should represent the energy of the exit channel relative to the Fermi level of the emitting nucleus. However, emission occurs from excited nuclei so that much of the influence of pairing and shell structure on the position of the ground state Fermi level should have washed out. Thus it would be more appropriate to use a separation energy measured relative to the excited

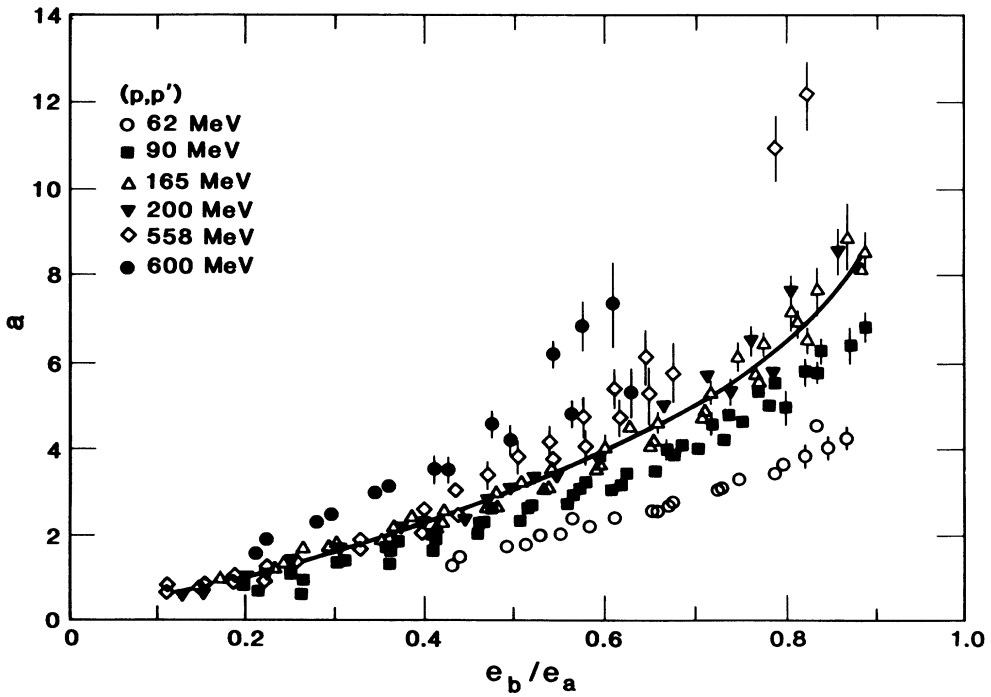

FIG. 2. Empirical slope values for (p,p′) reactions plotted as a function of the energy parameter ratio e_b/e_a. The curve shows the general trend of the results for 165 and 200 MeV incident protons.

state Fermi level in evaluating e_b.

To accomplish this change, the parameter e_b is replaced by $e_b' = \epsilon_b + S_b$ where the separation energy S_b is obtained from the liquid drop model with the pairing and shell terms neglected. Using the mass formula of Myers and Swiatecki[43] for spherical nuclei, the separation energy for a nucleus C into a particle b and a nucleus B is given by

$$S_b = 15.68(A_C - A_B) - 28.07\left[\frac{(N_C-Z_C)^2}{A_C} - \frac{(N_B-Z_B)^2}{A_B}\right] - 18.56(A_C^{2/3} - A_B^{2/3}) + 33.22\left[\frac{(N_C-Z_C)^2}{A_C^{4/3}} - \frac{(N_B-Z_B)^2}{A_B^{4/3}}\right] - 0.717\left[\frac{Z_C^2}{A_C^{1/3}} - \frac{Z_B^2}{A_B^{1/3}}\right] + 1.211\left[\frac{Z_C^2}{A_C} - \frac{Z_B^2}{A_B}\right] - I_b \ . \quad (4)$$

Here the subscripts C and B refer to the corresponding nuclei, the quantities N, Z, and A are the neutron, proton, and mass numbers of the nuclei, and I_b is the energy required to break the emitted particle up into its constituent nucleons.

A comparison of Figs. 1 and 3 shows that the parameter $e_b' = \epsilon_b + S_b$ indeed gives a more consistent description of the 90 MeV incident proton data than does e_b.

Other data systems are not as complete as the 90 MeV proton data and thus are not as sensitive to the choice of energy parameter. All seem to be adequately described using e_b', and this energy parameter has been adopted here.

C. Dependence on emitted particle type

The data from Fig. 3 have been replotted in Fig. 4 to compare the angular distribution slopes for the different particle types emitted from a single target. While all the results agree at the lower end of the energy scale, at higher energies the neutron results tend to be below the trend of the proton, deuteron, triton, and ^{3}He slopes, while the alpha particle results tend to be above them. This behavior seems quite general for nucleon induced reactions. For alpha-particle-induced reactions, this trend is not evident, but the data are more limited and their analysis is complicated by the presence of forward angle components.

D. Dependence on bombarding energy

When the angular distribution slopes for a single proton induced reaction at a variety of bombarding energies are plotted together, a second order dependence on bombarding energy becomes evident, as shown in Fig. 5. While there is general broad agreement between the points, the angular distribution slopes for a given bombarding energy begin to rise above the main trend line as the emission energy approaches its maximum.

The ^{54}Fe(α,α') data in Fig. 6, on the other hand, all fall on a single, well defined curve even though the measurements were done at two different laboratories. No bombarding energy dependence is observed.

VI. PARAMETRIZING THE ANGULAR DISTRIBUTION SLOPES

Only a subset of the available data was used in the parametrization so that the predictive ability of the final

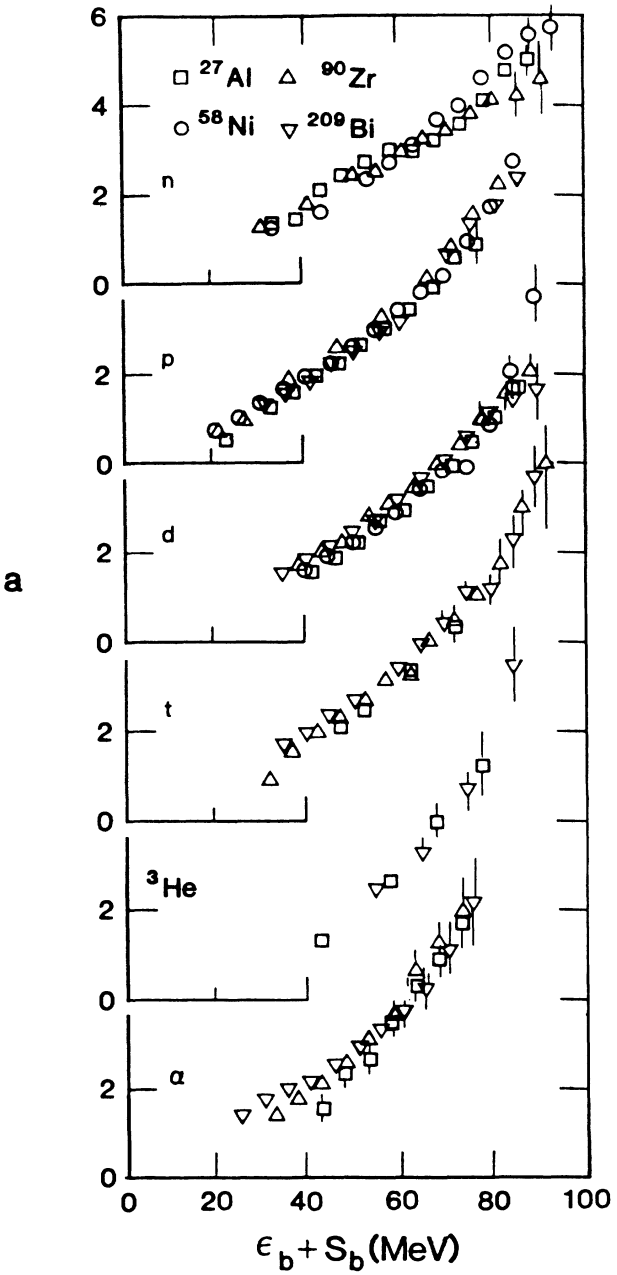

FIG. 3. Empirical slope values for reactions induced by 90 MeV protons shown vs the exit channel energy parameter $e_b' = \epsilon_b + S_b$. The different types of points refer to the four different target nuclides, and the results for each type of emitted particle are shown separately.

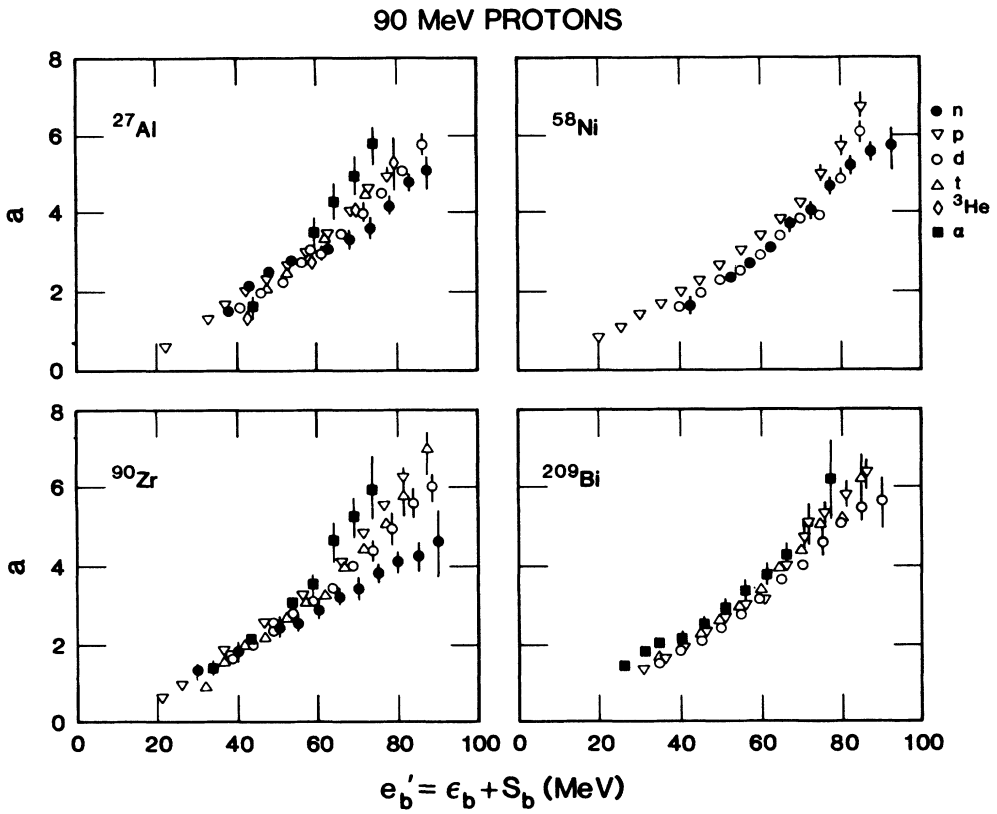

FIG. 4. Empirical slope values for reactions induced by 90 MeV protons shown vs the energy parameter e_b'. The different types of points refer to different emitted particles, and the results for each target nuclide are shown separately.

equations could be verified, and a concerted effort was made to limit the number of free parameters. Since the parametrization is only intended to reproduce global trends in the somewhat scattered slope values, a least squares fitting process was deemed unnecessary.

A. General behavior

The slope values, $a(e_b')$, have been described with a polynomial in e_b'. The leading term was assumed to be linear to guarantee that calculated angular distributions at $e_b'=0$ will be isotropic. With an energy parameter other than the channel energy itself, it is impossible to guarantee isotropy at zero emission energy, but the condition of isotropy for zero particle energy inside the emitting nucleus, is a good alternative.

Because of the second order dependences seen with incident protons and because of the change in the primary parameter at incident energies above 100 MeV, the process of parametrizing the general shapes of the angular distributions was begun with the ^{54}Fe(α,α') data shown in Fig. 6. These data lead to the relation

$$a(e_b')=0.040e_b'+1.8\times10^{-6}(e_b')^3 \quad (5)$$

which in turn was used to generate the curve shown in Fig. 6.

B. Incident nucleons at 35–100 MeV

Equation (5) must now be modified to account for the observed second order dependencies on bombarding energy and emitted particle for nucleon induced reactions.

The incident energy dependence is accounted for by adding a third term which varies as $(e_b'/e_a')^n$ where e_a' is the entrance channel analog of e_b'. The 39, 62, and 90 MeV (p,d) data were chosen to set this term, and the exponent was determined to have a value of 4. The results are shown in Fig. 5.

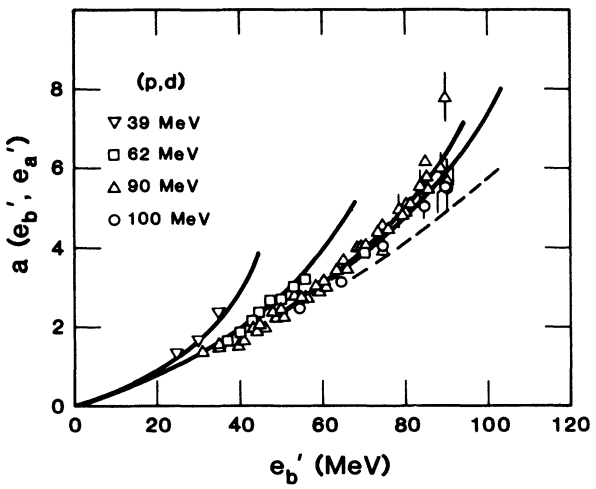

FIG. 5. Empirical and calculated slope values for (p,d) reactions at bombarding energies of 39–100 MeV. The empirical points are designated by bombarding energy. The solid curves are the result of the parametrization for proton-induced reactions, while the dashed curve shows the corresponding values for alpha particle-induced reactions.

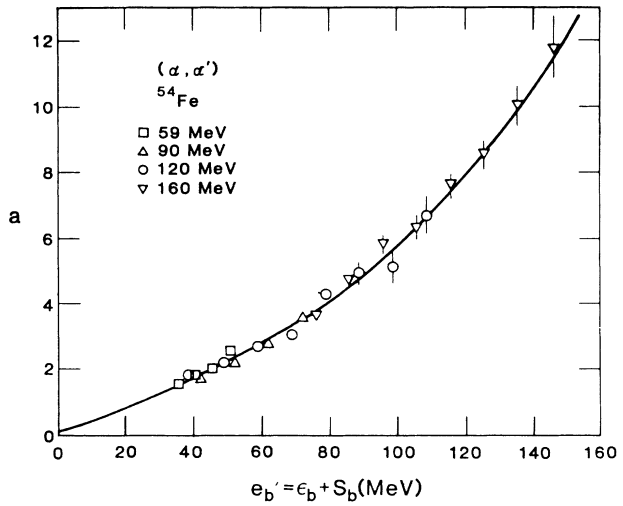

FIG. 6. Empirical slopes for inelastic scattering of 59–160 MeV alpha particles from ^{54}Fe. The different types of points are for different bombarding energies, while the curve shows the slopes calculated with the parametrization adopted for alpha-particle-induced reactions.

As a simple approximation to the second order dependence on the emitted particle, this third term in $a(e_b')$ is assumed to have the same normalization for proton, deuteron, triton, and ^{3}He angular distributions, while it is halved for neutrons and doubled for alpha particles. The scatter in the experimental results does not permit a determination more accurate than one based on ratios of small whole numbers.

For incident neutrons the slopes of the 60 MeV (n,p) angular distributions were found to be better reproduced using the three term expression rather than the two term one. The third term will therefore be used for all nucleon induced reactions.

Taking into account both the projectile and emitted particle dependences, the slope parameter for the angular distributions can be written as

$$a(e_b')=0.040e_b'+1.8\times10^{-6}(e_b')^3 + 1.9M_a m_b(e_b'/e_a')^4 , \quad (6)$$

where

$$M_\alpha=0 , \quad M_n=M_p=1 , \quad m_n=\tfrac{1}{2} , \quad (7a)$$

$$m_p=m_d=m_t=m_{^3He}=1 , \quad m_\alpha=2 , \quad (7b)$$

C. Incident nucleons above 150 MeV

To avoid a whole new parametrization for nucleon induced reactions in the regime above 150 MeV, the parameter e_b' in the first two terms of Eq. (6) is replaced by

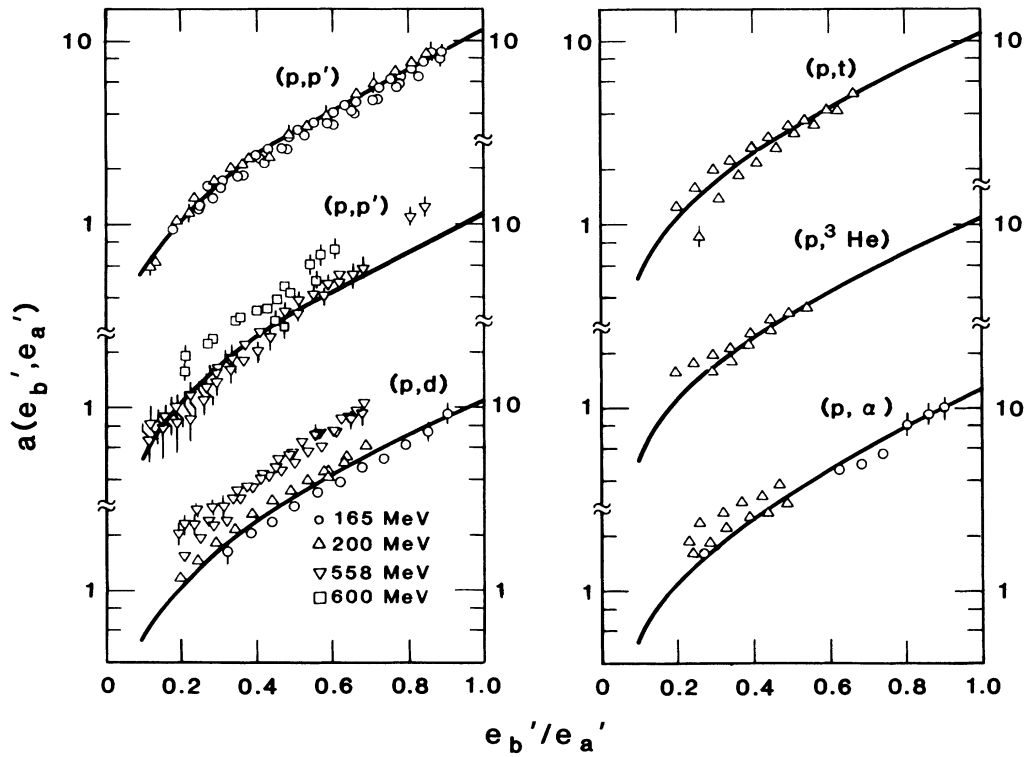

FIG. 7. Empirical and calculated slope values for proton-induced reactions at bombarding energies greater than 100 MeV. The empirical points are designated by bombarding energy for each reaction type. The solid curves are the result of the parametrization adopted for proton-induced reactions.

the ratio

$$X_1=(E_1 e_b'/e_a')\ , \tag{8a}$$

where

$$E_1=\min(e_a',E_{t1}) \tag{8b}$$

and E_{t1} is the energy at which the transition is made from an e_b' dependence to an e_b'/e_a' dependence. For incident energies below the transition point, the previous results are recovered, and the only new parameter is the transition energy which must lie between 100 and 165 MeV.

A value of E_{t1} of around 130 MeV was found from the 165 and 200 MeV (p,p') data. To distinguish between the assumed sharp transition and a more gradual one, a lot of good angular distribution data is needed for incident energies between 100 and 150 MeV. Figure 7 shows that all of the 165 and 200 MeV data plus the 558 MeV (p,p') data follow the same trends, while the 600 MeV (p,p') and the 558 MeV (p,d) reactions have higher slope values.

D. Incident nucleons below 40 MeV

While isotropy is now guaranteed as e_b' approaches zero, the third term in Eq. (6) can cause the angular distribution slopes to jump by an unrealistically large amount in a very small interval of emission energies. To deal with this problem, the third term was recast to give it the same form as the first two, but with a lower transition energy, E_{t3}. For values of e_a' below E_{t3}, the third term and, indeed, the slopes of the angular distributions thus depend on the emission energy but not the incident energy.

Six (nucleon-nucleon) angular distributions were calculated in Ref. 1 to be at least 90% multistep direct emission. Together they indicate a transition energy of about

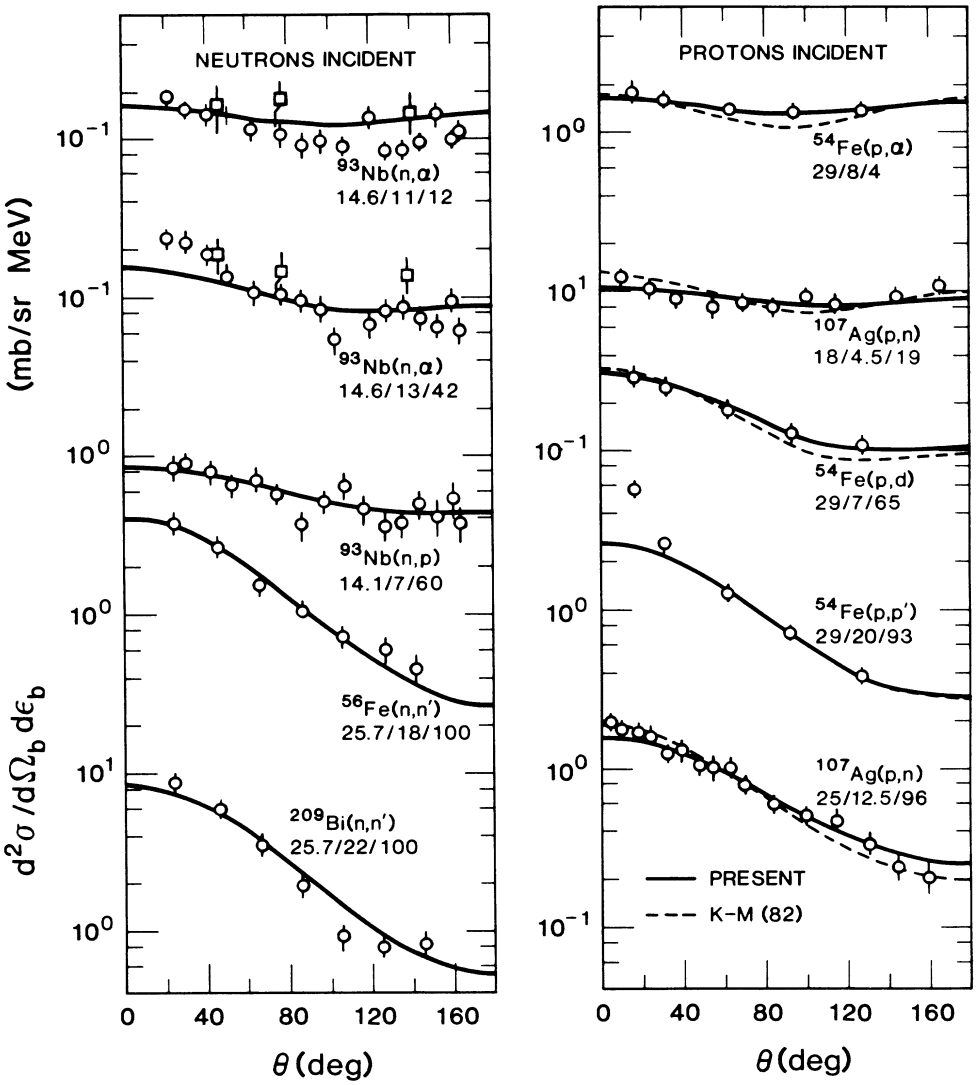

FIG. 8. Comparison of experimental and calculated angular distributions for nucleon-induced reactions at energies less than 35 MeV. The points show the data, the solid curves are the results of this work, and the dashed curves are the corresponding KM results (Ref. 2). Each angular distribution is labeled by the reaction, the incident laboratory energy, the emitted channel energy, and the percent of the cross section which is believed to be multistep direct.

41 MeV. Thus the final formula for the slope parameters is

$$a(e_b',e_a')=0.040X_1+1.8\times10^{-6}(X_1)^3 +6.7\times10^{-7}M_a m_b(X_3)^4 , \quad (9)$$

where X_3 is defined analogously to X_1.

VII. COMPARISON OF PARAMETRIZATION WITH DATA

A parametrization is only useful if it successfully accounts for the data not used in setting the parameter values.

A small computer program was written to calculate angular distributions for all of the systems listed in Tables I–III except those for the 720 MeV (α,p) reactions, for which the needed parameter E_{t1} is unknown. The program uses the liquid drop model binding energies of Eq. (4) to calculate the parameters e_a' and e_b', Eqs. (7), (8), and (9) for the slope parameter, and Eq. (3) for the angular distributions. The results have been compared to the measured center-of-mass angular distributions, with the normalization $d\sigma/d\epsilon_b$ adjusted to facilitate comparison with the data. For the systems used in the KM studies, the fractions, $f_{\rm MSD}$, of multistep direct emission from that work were employed. All other angular distributions were chosen to be pure MSD.

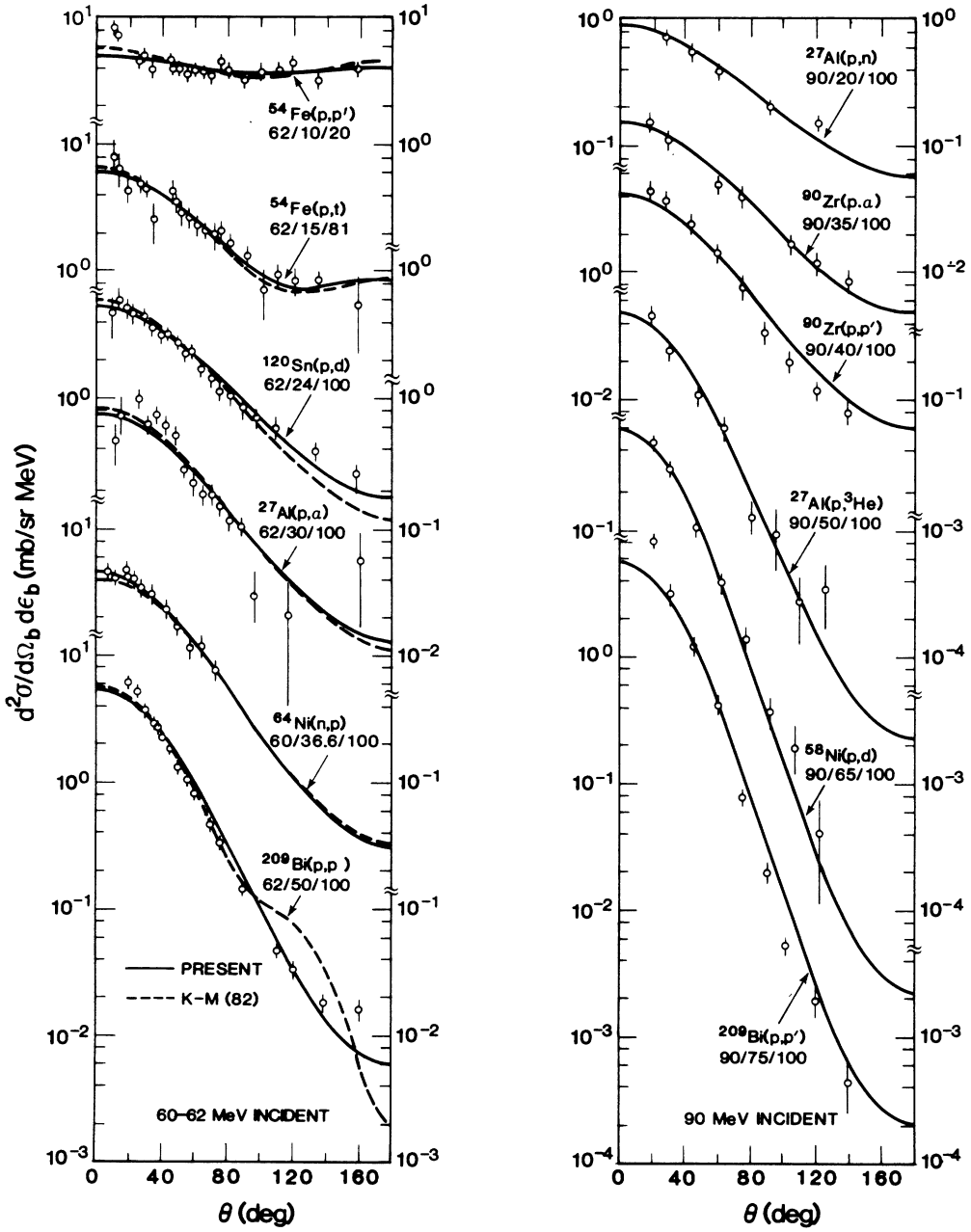

FIG. 9. Comparison of experimental and calculated angular distributions for reactions induced by 60–90 MeV nucleons. The points, solid curves, dashed curves, and labels are as in Fig. 8.

A. Nucleon-induced reactions below 300 MeV

The primary interest in this work is in nucleon-induced reactions at incident energies up to 200 MeV. These reactions show slightly different systematics in each of three domains of incident energy. Figure 8 shows the results for incident energies below 35 MeV (or e_a' below $E_{t3}=41$ MeV) where the angular distributions are independent of the incident energy. Figure 9 covers incident energies of 62 and 90 MeV for which e_a' is between E_{t3} and $E_{t1}=135$ MeV and there is a second order dependence on this parameter. Figure 10 shows results for incident energies of 165 and 200 MeV, where the energy parameter describing the angular distributions is e_b'/e_a'.

In each of the three figures, the level of agreement between experiment and calculation is quite good. Nor is there any significant difference in the quality of the fits between the systems that were and were not used in the earlier phases of this work.

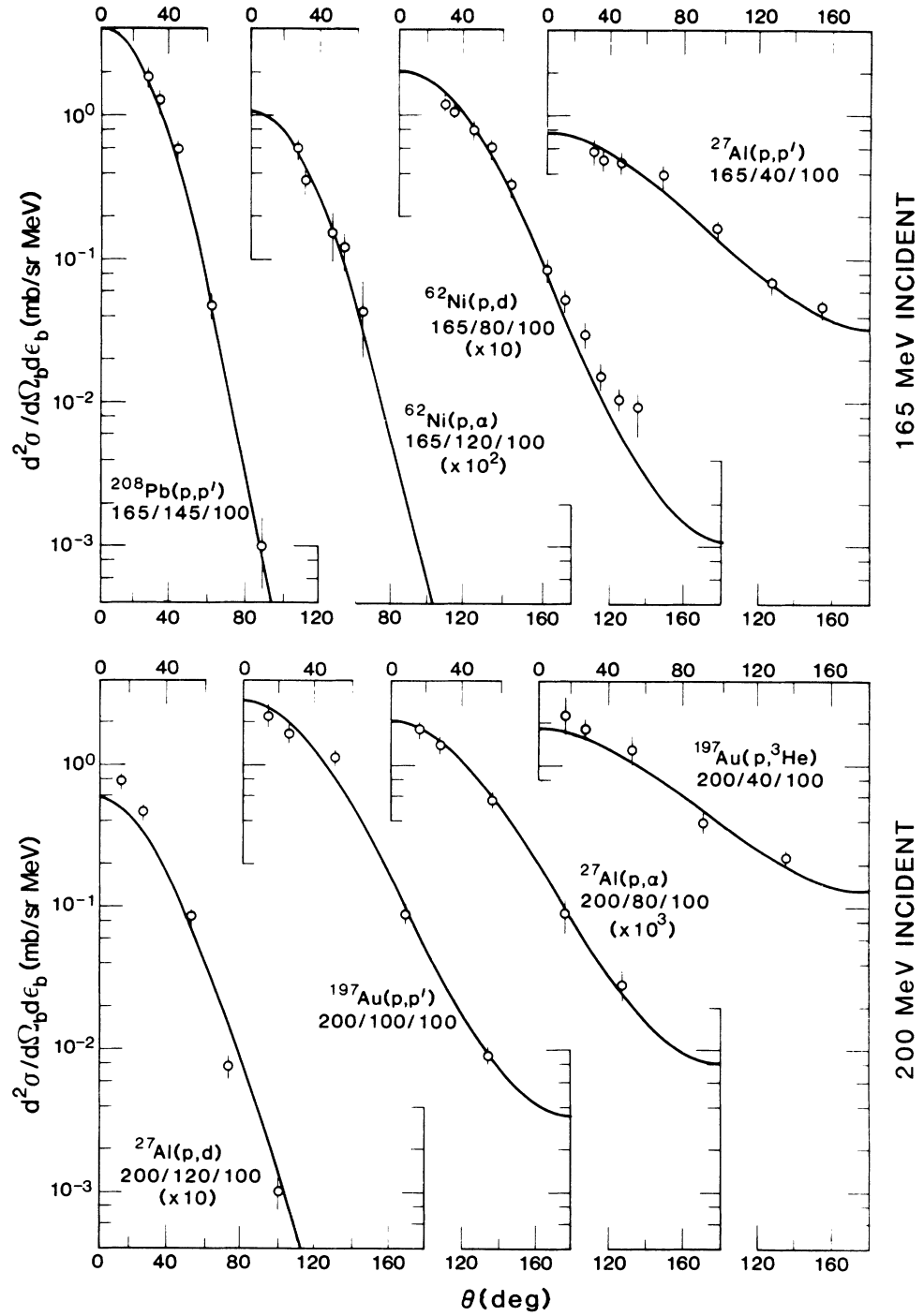

FIG. 10. Comparison of experimental and calculated angular distributions for reactions induced by 165 and 200 MeV protons. The points, solid curves, and labels are as in Fig. 8.

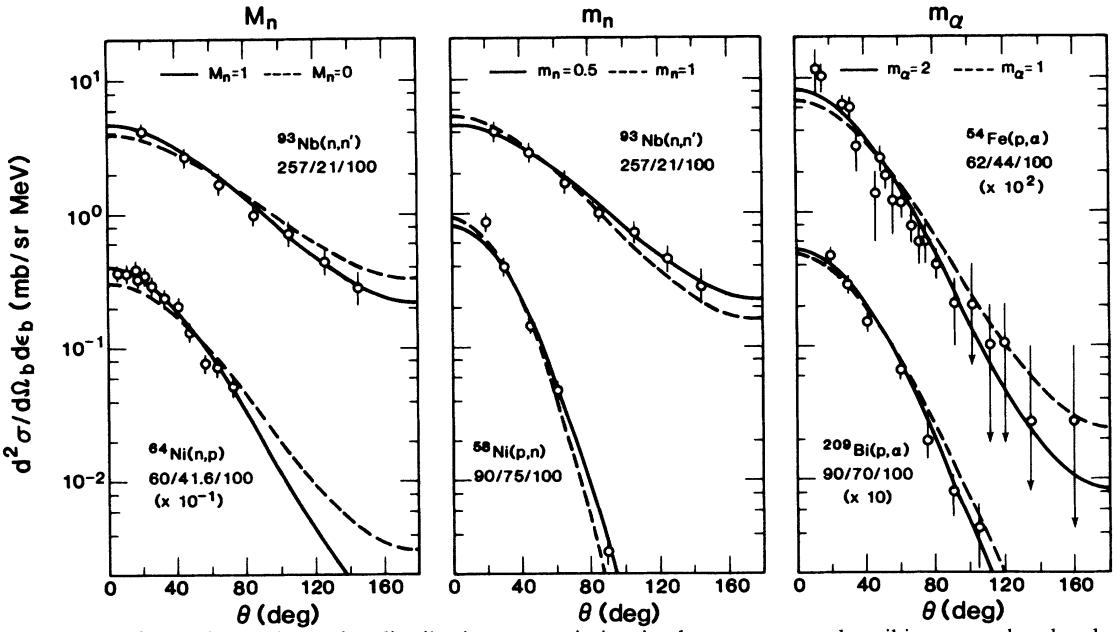

FIG. 11. Sensitivity of experimental angular distributions to variation in the parameters describing second order dependences. The points show the data, the solid curves give the results of the present work with the adopted values of all the parameters, and the dashed curves give the results when one of the parameters is varied as indicated.

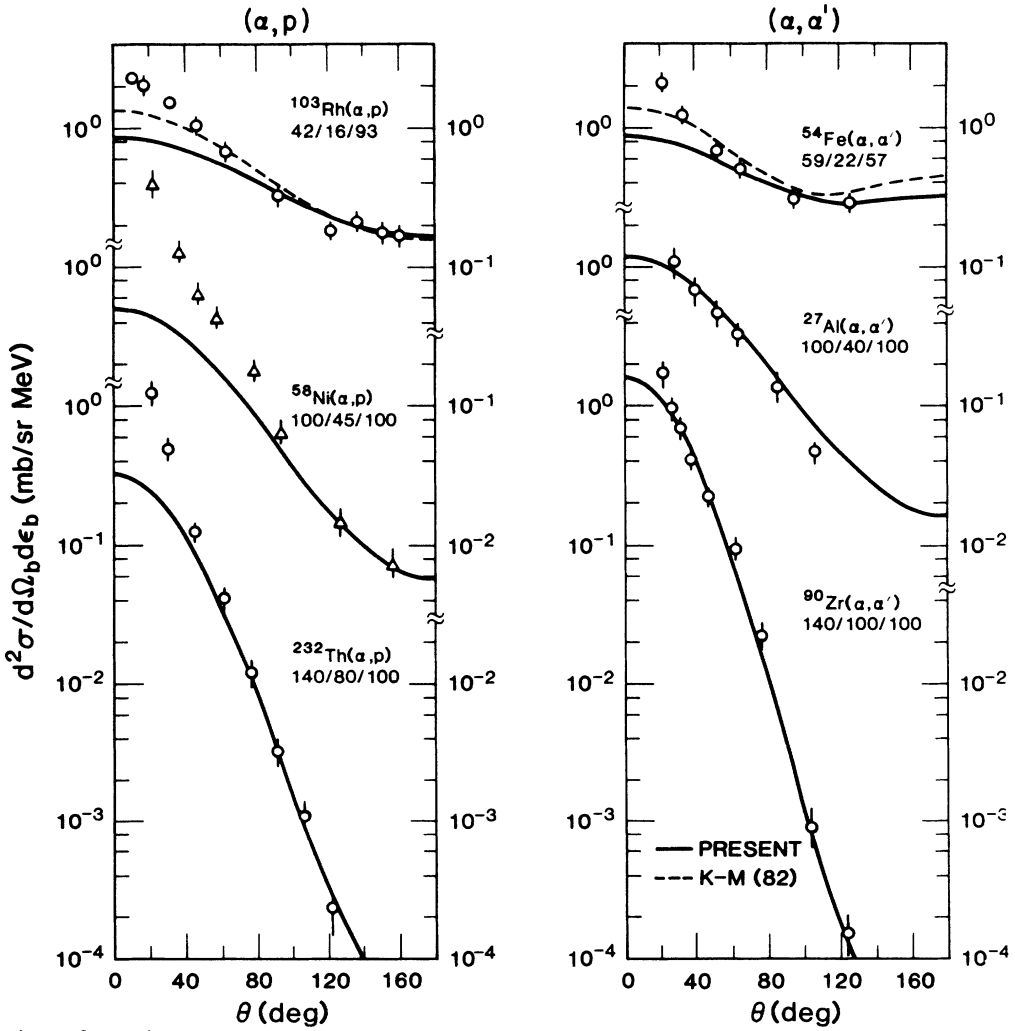

FIG. 12. Comparison of experimental and calculated angular distributions for (α,p) and (α,α') reactions. The points, solid curves, dashed curves, and labels are as in Fig. 8.

An important result from these figures is the applicability of the current parametrization for multistep compound emission. The angular distributions shown in Fig. 8 range from 4% to 100% MSD, and the good fits suggest that the assumption made in Sec. III regarding the functional form of the MSC component is both reasonable and adequate.

Figures 8 and 9 also show angular distributions from the KM systematics[2] with the energy parameter $e_b = \epsilon_b + B_b$. The current results are on average at least as good at reproducing the data, and the results in Fig. 8 imply that they are somewhat superior at low emission energies.

The most noteable disagreements seen are for 62 MeV protons incident on ^{12}C. Here the inelastic proton angular distributions at 30 and 40 MeV are found to have nearly identical shapes at forward angles, with only the 40 MeV data accounted for by the systematics. The ^{12}C(p,α) reaction at an emission energy of 30 MeV displays bumps of extra cross section at angles forward of 40° and backward of 140°. This is quite possibly related to the alpha cluster substructure of the target.

A much smaller difficulty is seen in the 90 MeV (p,p′) angular distributions. For all of the targets except ^{27}Al, the angular distributions for channel energies greater than 40 MeV are better reproduced using an effective channel energy which is 5 MeV higher than the real one. Other exit channels do not show this effect, nor do (p,p′) results from lower or higher bombarding energies.

B. Sensitivity to parameter values

The third term in Eq. (9) has two multipliers: M_a which is a function of the projectile and m_b which is a function of the emitted particle. Of the three values of M_a which have been assigned, the values $M_\alpha = 0$ and $M_p = 1$ simply reflect the origin of the third term in the equations for a. Thus only M_n is an adjustable parameter and only values of 0 and 1 were considered. Similarly, for m_b, variations from unity were only considered for m_n and m_α, and then only in ratios of small whole numbers.

Figure 11 shows the sensitivity of the data to using $M_n = 0$ instead of 1 and to chosing $m_n = m_\alpha = 1$ instead of the adopted values of $\frac{1}{2}$ and 2, respectively. In each case there is a small but decided preference for the adopted values. Thus, the main argument in support of the proposed values of M_n, m_n, and m_α comes from the accumulated weight of weak but consistent evidence from a number of reactions.

C. Alpha-particle-induced reactions below 200 MeV

For incident alpha particles, the systematics appear to be simpler than those for incident nucleons, but the additional forward angle components make the fits to the data look less impressive. In the original KM work, the presence of these extra components was not recognized, and the parametrization was designed to reproduce all of the data points. this is why it was possible to use the same

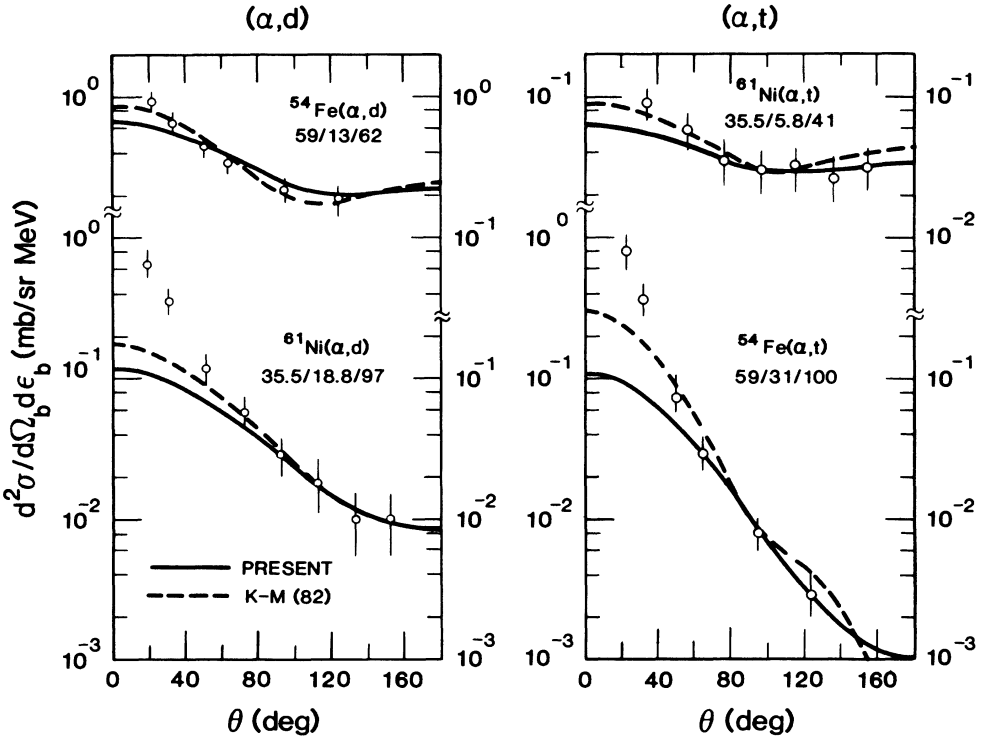

FIG. 13. Comparison of experimental and calculated angular distributions for (α,d) and (α,t) reactions. The points, solid curves, dashed curves, and labels are as in Fig. 8.

parametrization for both proton- and alpha-particle-induced reactions.

In Figs. 12 and 13, the present results have generally been normalized to the data at the more backward angles. The corresponding KM results[2] (which have occasionally been renormalized downward) are also included.

Using the present parametrization, the fits to the angles that are free of the forward angle components are generally quite good, but there are a few exceptions. The ^{61}Ni(α,α') reaction data at 35.5 MeV show a rise at back angles, even at emission energies where the cross section should be pure multistep direct. For the 100 MeV (α,α') data on ^{25}Mg and ^{27}Al (the only targets used), the angular distributions get steeper at back angles than at forward angles. No other data do this, and it is possible that too much background was subtracted. The 140 MeV (α,α') angular distributions for reactions on ^{27}Al and ^{58}Ni are better reproduced if the energy parameter is arbitrarily increased by about 10 MeV. Finally, the 100 MeV (α,p) angular distributions for reactions on ^{27}Al and ^{58}Ni show empirical slopes well above the general systematics and are not reproduced by the present parametrization.

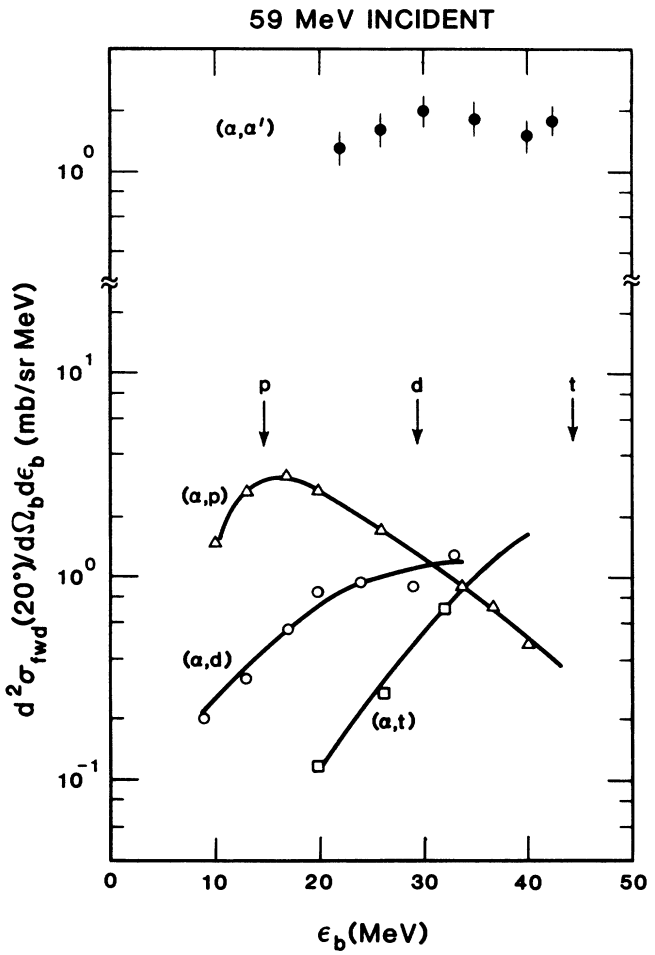

FIG. 14. Energy spectra of the excess 20° cross section for reactions of 59 MeV alpha particles with ^{54}Fe. The arrows show the emission energies which correspond to the beam velocity for proton, deuteron, and triton emission. The curves are intended simply to guide the eye.

(Heavier targets were not employed.) This probably reflects an inability to resolve the "main" component from a quite dominant "forward angle" component. The present results for these systems were generally normalized to the data taken backwards of 115°. To probe the origin of the forward angle components, it is instructive to study the cross section in excess of the present results.

The angular distributions of the extra forward angle cross section show very little variation with either incident or outgoing energy, although the uncertainties are quite large. In general, their slope parameters would normally correspond to values of e_b' around 100–140 MeV.

The energy distributions are more instructive. Figures 14 and 15 show the 20° spectra of the excess cross section for some sample reactions.

For the (α,p) reactions and the few (α,d) and (α,t) cases that have been studied the spectra peak at an energy roughly corresponding to the beam velocity, suggesting some variety of breakup mechanism.[44–48] The (α,α') forward angle components are relatively flat across a given energy spectrum. They increase rapidly in intensity with target mass at 140 MeV (not even being seen for the aluminum and nickel targets), and decrease in intensity with increasing bombarding energy, suggesting a possible correlation with the elastic scattering peak. Clearly a detailed investigation of these components is needed but is outside the scope of this paper.

D. Proton-induced reactions above 300 MeV

While the data at incident energies above 300 MeV are too fragmentary for definitive analysis, it is still interesting to compare them to the current systematics.

Figures 16 and 17 show such comparisons. As expect-

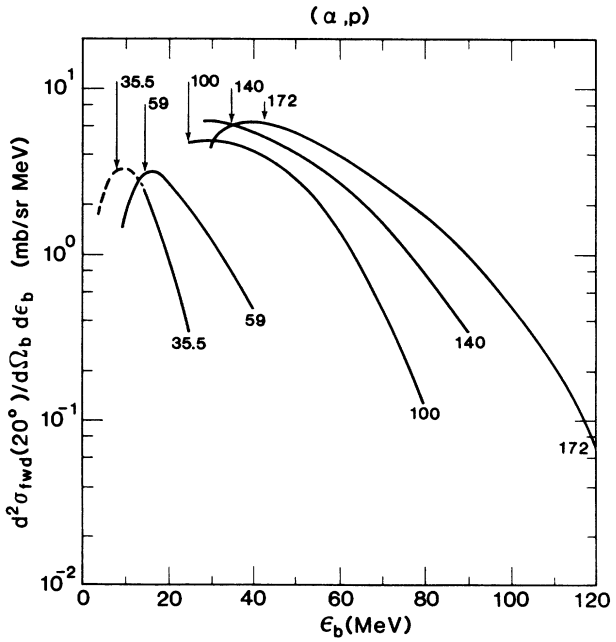

FIG. 15. Energy spectra of the excess 20° (α,p) cross section at various bombarding energies. The curves show the trends of the data, and the arrows indicate the emission energies which correspond to the beam velocity.

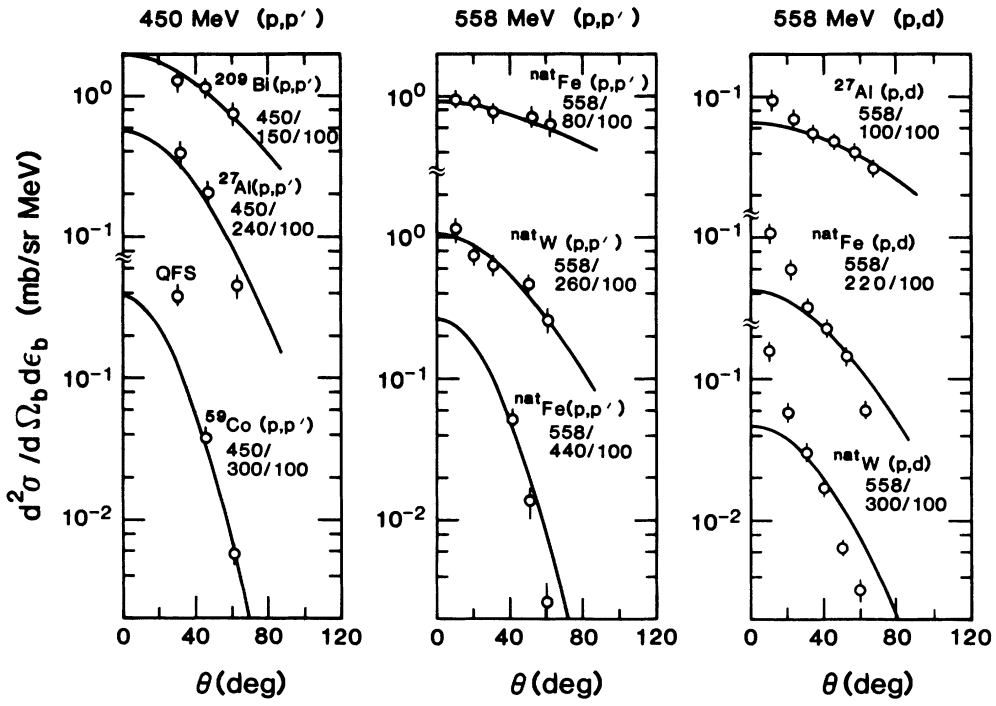

FIG. 16. Comparison of experimental and calculated angular distributions for reactions induced by 450 and 558 MeV protons. The points, curves, and labels are as in Fig. 8.

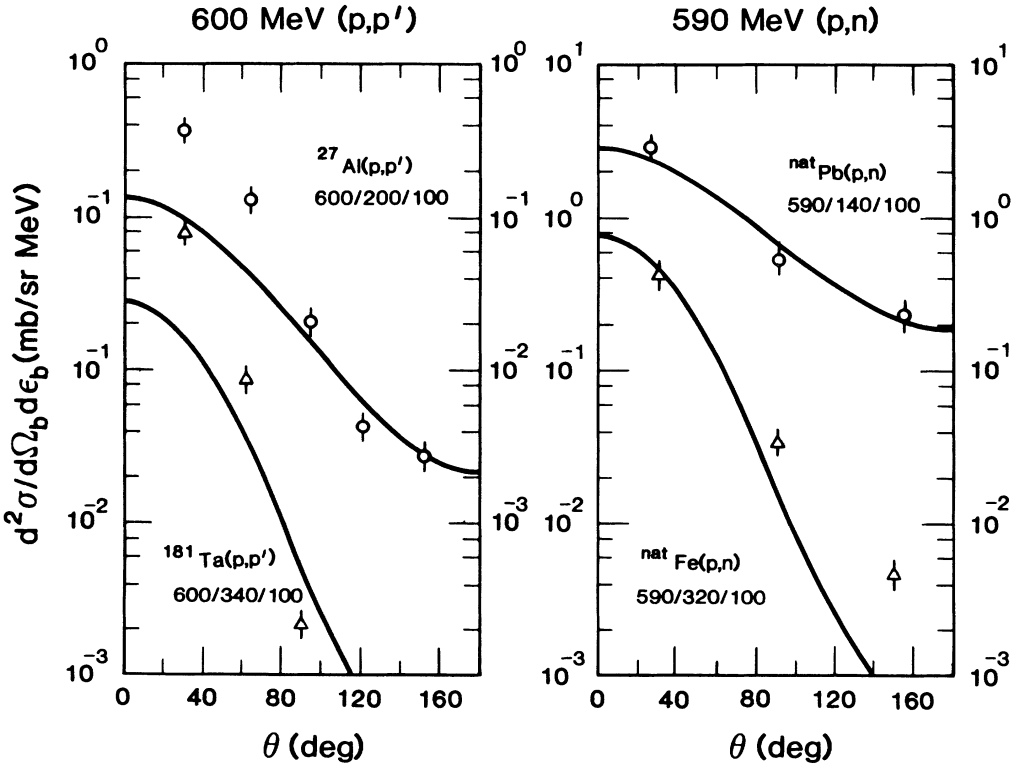

FIG. 17. Comparison of experimental and calculated angular distributions for reactions induced by 590 and 600 MeV protons. The points, curves, and labels are as in Fig. 8.

ed from the results in Fig. 7, the 558 MeV (p,p′) angular distributions can be well reproduced, while the systematics seriously underpredict the steepness of the 558 MeV (p,d) and the 600 MeV (p,p′) curves. The fragmentary angular distributions for the 450 MeV (p,p′) reactions are also seen to be at least qualitatively consistent with the calculated curves. Finally for the 590 MeV (p,n) data, the angular distributions sketched out by the data tend to be roughly consistent with the systematics, but for ϵ_b above about 200 MeV, the 150° experimental cross section begins to rise above the calculated curves.

E. Deuteron-induced reactions

Deuteron-induced reactions have not been studied here because of the expected significant contributions from projectile breakup processes. However, because of the success of the KM systematics, it is interesting to see how well the present parametrization can do. The data[32,49] used are listed in Table IV.

It is assumed that $M_d=1$ and $E_{t3}=41$ MeV as for incident nucleons. The value of E_{t1} would be expected to be at least 130 MeV (the proton value), but is not needed at the available incident energies.

Figure 18 shows that, perhaps surprisingly, the present results account quite well for the 25 MeV data, except, of course, for the breakup cross section in the proton channel. The effect of the third term in Eq. (9) is crucial in this regard. For the ^{63}Cu(d,α) reaction with an emission channel energy of 27.8 MeV, replacing $M_d=1$ with $M_d=0$ would produce an angular distribution significantly flatter than the KM result shown.

Figure 19 shows the comparisons of the present systematics with the data[49] taken at 70 and 80 MeV. The data for the aluminum, nickel, and zirconium targets are all well reproduced (again, except for proton angular dis-

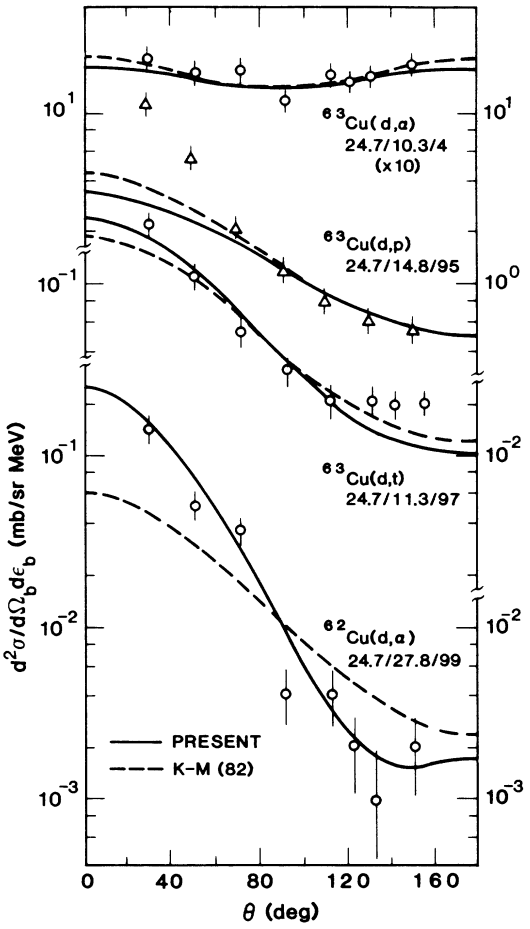

FIG. 18. Comparison of experimental and calculated angular distributions for reactions induced by 24.7 MeV deuterons. The points, curves, and labels are as in Fig. 8.

TABLE IV. Data for inclusive deuteron-induced reactions.

Reaction	Target	Proj. energy (MeV)	Channel energies Range (MeV)	No.	No. fit	Lab. angles Range (deg)	No.	Ref.
(d,p)	Cu	25	4.3–24.8	3		30–150	7	32
(d,p)	Al	80	60	1		30–150	7	49
(d,p)	Pb	70	50	1		20–140	9	49
(d,d′)	Cu	25	5.3–18.8	3		30–150	9	32
(d,d′)	Al,Ni	80	30,50	2		20–150	7–8	49
(d,d′)	Pb,Th	70	20–60	7		20–140	8–9	49
(d,t)	Cu	25	5.8–18.3	3		30–150	9	32
(d,t)	Al,Ni	80	20,40	2		20–150	7–8	49
(d,t)	Zr,Th	70	30,40	2		20–150	8	49
(d,α)	Cu	25	10.3–27.8	3		30–150	8	32
(d,α)	Al,Ni	80	40–60	6		20–150	7–8	49
(d,α)	Zr-Th	70	20–50	10		20–150	8–9	49
	Total ($E_{inc}<300$ MeV)			43				

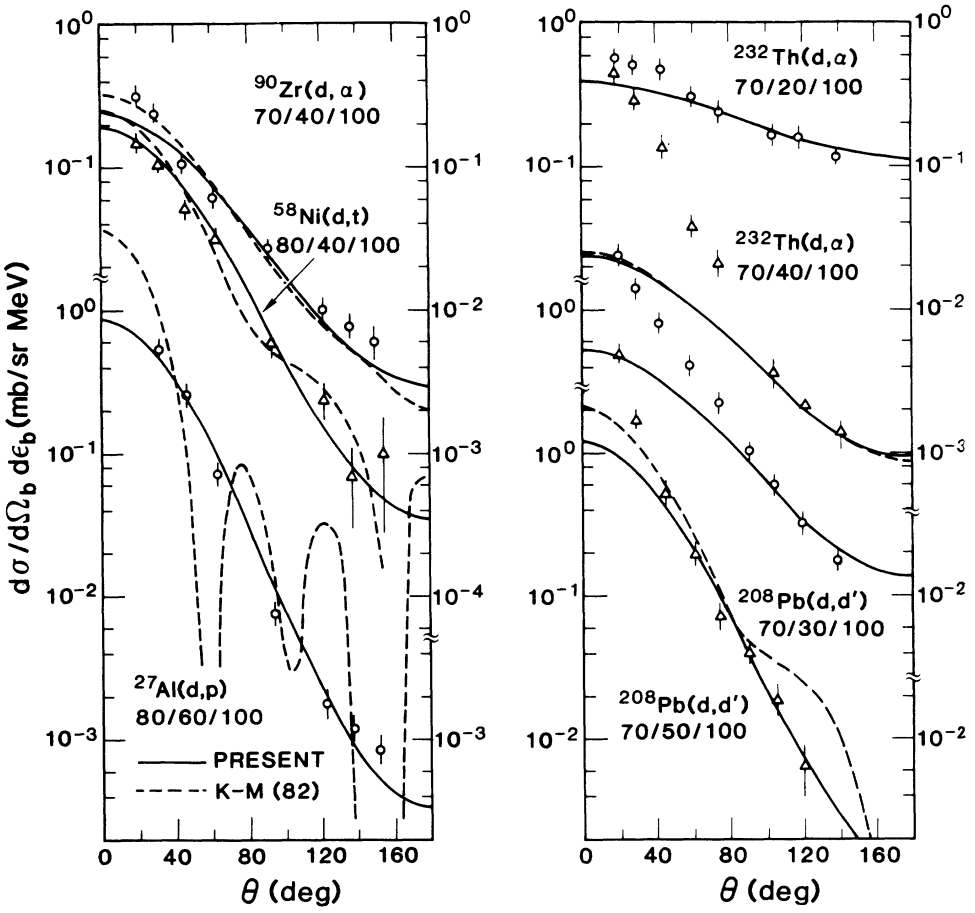

FIG. 19. Comparison of experimental and calculated angular distributions for reactions induced by 70 and 80 MeV deuterons. The points, curves, and labels are as in Fig. 8.

tributions for energies on the breakup peak). The fits are generally comparable to those obtained from the KM systematics using the energy parameter e_b, but avoid the wild oscillations at the higher emission energies. On the other hand, the data for lead and thorium show significant forward angle cross section that is not accounted for.

A possible mechanism to explain the extra cross section would be normal preequilibrium reactions induced by one of the breakup nucleons. This is, of course, only speculation, but in many cases the present parametrization for reactions induced by neutrons with half the beam energy can at least qualitatively account for the angular dependence of the extra cross section.

VIII. SUMMARY AND CONCLUSIONS

The present work extends the range of applicability of the earlier Kalbach-Mann systematics to higher bombarding energies and improves their behavior at very low emission energies. This has been accomplished without dramatically increasing the number of adjustable parameters, and at the same time some useful insights have been gained into the special intricacies of complex particle induced reactions. The key to the success of this work was the use of a simple exponential in $\cos\theta$ to describe the angular dependence from multistep direct processes.

A. General systematics

The present work confirms the KM result that for bombarding energies less than 100 MeV, the main physical parameter determining the shape of the angular distributions is the energy of the emitted particles. The most consistent description of the data occurs when this energy is combined with a liquid drop model separation energy from which the pairing and shell effects have been removed.

For incident protons (and presumeably neutrons) with energies above 130 MeV, the systematics change and the angular dependence of the cross sections is determined by the ratio of the energies in the entrance and exit channels of the reaction. If such a transition occurs for alpha-particle-induced reactions, it does so above 172 MeV.

Many of the angular distributions for alpha-particle-induced reactions have at least two components: the main component corresponding to the usual preequilibrium cross sections and a much more forward-peaked component which is probably due to some variety of breakup process.

Finally, some second order dependencies were observed when the emission energy approaches the incident energy. The alpha projectile results tend to be flatter than those for nucleon or deuteron projectiles, and they do not show the small incident energy dependence seen in

those reactions at energies below the 130 MeV transition point. In addition the nucleon and deuteron projectile data show a weak dependence on the nature of the emitted particle, with the neutron angular distributions being somewhat flatter and the alpha particle results somewhat steeper than those for p, d, t, or ^{3}He emission.

B. Parametrization

As was the case with the KM systematics, the angular distribution parametrization derived here can in no sense be considered to be unique. It can only be considered as appropriate and useful.

The new formulae for calculating continuum angular distributions in light particle induced reactions are summarized in the following equations as

$$\frac{d^2}{d\Omega\, d\epsilon_b}=\frac{1}{4\pi}\frac{d\sigma}{d\epsilon_b}\frac{a}{\sinh(a)}[\cosh(a\cos\theta)+f_{\mathrm{MSD}}\sinh(a\cos\theta)]\ ,$$

$$a(e_b',e_a')=C_1X_1+C_2(X_1)^{n2}+C_3M_am_b(X_3)^{n3}\ , \tag{10}$$

$$X_1=(E_1e_b'/e_a')\ ,$$

$$X_3=(E_3e_b'/e_a')\ , \tag{11}$$

$$E_1=\min(e_a',E_{t1})\ ,$$

$$E_3=\min(e_a',E_{t3})\ , \tag{12}$$

$$e_b'=\epsilon_b+S_b\ . \tag{13}$$

The quantity e_a' is defined analogously to Eq. (13) and the separation energies S_a and S_b are given by Eq. (4).

The values of the parameters in the above equations are given in Table V along with the number of angular distributions that were used to determine them. Note that of all the parameters listed in the table only five are continuously variable. The two exponents were required to be integers, while M_a and m_b were constrained to be ratios of small whole numbers.

This list compares with four continuous variables and two integer exponents in the KM systematics. If the present systematics were constrained to the same range of bombarding energies, the parameter E_{t1} could be omitted and the number of parameters would be the same as in the earlier study except for the M_a and m_b values which represent second order effects too weak to be seen there.

C. Perspectives

The parametrization described here successfully accounts for a wide variety of experimental angular distributions, including those that were used neither to study the systematics nor to set the parameter values. For systems which were considered in the earlier KM systematics, the present results provide comparable or better agreement with the data. Thus the high energy threshold of the KM systematics has been extended from 60 to 200 MeV and perhaps higher. (Data at higher bombarding energies are scarce, and results for 450–600 MeV proton induced reactions are mixed.)

For a complete description of continuum angular dis-

TABLE V. Summary of parameter values.

Parameter	Value	No. angular distributions used[a]
n_2	3	24
n_3	4	56
C_1	0.04	(24)
C_2	1.8×10^{-6}	(24)
C_3	6.7×10^{-7}	(56)
E_{t1}	130±10 MeV	65
E_{t3}	41±5 MeV	6
M_{n}	1	13
M_{p}	1	From definition of C_3
M_{d}	1	Assumed
M_α	0	From definition of C_1,C_2
m_{n}	$\frac{1}{2}$	32
m_{p}	1	[b]
m_{d}	1	From definition of C_3
m_{t}	1	[b]
$m_{^3\mathrm{He}}$	1	[b]
m_α	2	21
Total used		217
data set ($E_{\mathrm{inc}}<300$ MeV)		750
Full Data set		913

[a]Values in parentheses mean that these angular distributions were also used for determining one or more previously listed parameters.

[b]Variation of this parameter was not considered.

tributions it will be necessary to include additional components. For incident alpha particles (and deuterons) there is a need to describe the cross section due to breakup processes, while for nucleon-induced reactions above 100 MeV quasifree scattering must be considered. Additional work on both mechanisms is needed, and the present systematics may help to separate these components from the main preequilibrium cross section in the data.

On the experimental side, there is clearly a need for more data at bombarding energies between 200 and 600 MeV. Each data set should optimally include energy spectra for several emitted particle types, each taken over a wide range of angles (preferably at increments of 15° or less) on a variety of targets. This would enable the current results to be tested and modified at the higher energies.

Finally, it is hoped that the present results will stimulate new theoretical work. The basic KM systematics are still unexplained after seven years of use. In addition there is the newly recognized change in energy parameter at incident nucleon energies of around 130 MeV. Could this be related to the threshold for pion production? If so, should we expect to see other "particle physics" phenomena, like the $\Delta(1236)$ resonance, influence the results at still higher bombarding energies? The systematics only tell us what is going on, but we still need to learn why.

ACKNOWLEDGMENTS

This work was performed under a consulting agreement with Los Alamos National Laboratory. The author is happy to acknowledge the hospitality of the Duke University Physics Department and the Triangle Universities Nuclear Laboratory. Dr. F. E. Bertrand, Dr. C. C. Chang, Dr. H. Machner, and Dr. R. E. Segel materially aided this work by providing copies of their data. Thanks are also due to Dr. Michael Bozoian and Dr. P. G. Young for critiquing this manuscript.

[1]C. Kalbach and F. M. Mann, Phys. Rev. C **23**, 112 (1981).
[2]C. Kalbach, Phys. Rev. C **25**, 3197 (1982).
[3]G. Mantzouranis, H. A. Weidenmüller, and D. Agassi, Z. Phys. A **276**, 145 (1976); G. Mantzouranis, Phys. Rev. C **14**, 2018 (1976).
[4]J. M. Akkermans, Phys. Lett. **82B**, 20 (1979); J. M. Akkermans, H. Gruppelaar, and G. Reffo, Phys. Rev. C **22**, 73 (1980).
[5]Sun Ziyang, Wang Shunuan, Zhang Jinshang, and Zhuo Yizhong, Z. Phys. A **305**, 61 (1982).
[6]C. Costa, H. Gruppelaar, and J. M. Akkermans, Phys. Rev. C **28**, 587 (1983).
[7]Akira Iwamoto and Kichinosuke Harada, Nucl. Phys. **A419**, 472 (1984).
[8]Kenichi Sato, Phys. Rev. C **32**, 647 (1985).
[9]A. De, S. Ray, and S. K. Ghosh, J. Phys. C **11**, L79 (1985).
[10]A. Chatterjee and S. K. Gupta, Z. Phys. A **313**, 93 (1983).
[11]M. Blann, W. Scobel, and E. Plechaty, Phys. Rev. C **30**, 1493 (1984).
[12]T. Tamura, T. Udagawa, D. H. Feng, and K.-K. Kan, Phys. Lett. **66B**, 109 (1977); T. Tamura, T. Udagawa, and H. Lenske, Phys. Rev. C **26**, 379 (1982).
[13]H. Feshbach, A. Kerman, and S. Koonin, Ann. Phys. **125**, 429 (1980).
[14]C. Kalbach, Los Alamos National Laboratory Report LA-UR-87-4139, 1987.
[15]C. Kalbach, Phys. Rev. C **23**, 124 (1981); **24**, 819 (1981).
[16]A. Marcinkowski, R. W. Finlay, G. Randers-Pehrson, C. E. Brient, and J. E. O'Donnell, Nucl. Phys. **A402**, 220 (1983).
[17]G. Traxler, A. Chalupka, R. Fischer, B. Strohmaier, M. Uhl, and H. Vonach, Nucl. Sci. Eng. **90**, 174 (1985).
[18]C. M. Castaneda, J. L. Ullman, F. P. Brady, J. L. Romero, N. S. P. King, and M. Blann, Phys. Rev. C **28**, 1493 (1983).
[19]R. Fischer, C. Derndorfer, B. Strohmaier, and H. Vonach, Ann. Nucl. Energy **9**, 409 (1982).
[20]S. M. Grimes, R. C. Haight, and J. D. Anderson, Phys. Rev. C **17**, 508 (1978).
[21]C. Kalbach, S. M. Grimes, and C. Wong, Z. Phys. A **275**, 175 (1975).
[22]S. M. Grimes, J. D. Anderson, and C. Wong, Phys. Rev. C **13**, 2224 (1976).
[23]A. M. Kalend, B. D. Anderson, A. R. Baldwin, R. Madey, J. W. Watson, C. C. Chang, H. D. Holmgren, R. W. Koontz, J. R. Wu, and H. Machner, Phys. Rev. C **28**, 105 (1983).
[24]D. Filges, S. Cierjacks, Y. Hino, A. W. Armstrong, and P. Cloth, Kernforschungsanlage, Julich, Report Jul-1960, 1984.
[25]F. E. Bertrand and R. W. Peelle, Phys. Rev. C **8**, 1045 (1973).
[26]J. R. Wu, C. C. Chang, and H. D. Holmgren, Phys. Rev. C **19**, 698 (1979).
[27]R. E. Segel, T. Chen, L. L. Rutledge, Jr., J. V. Maher, John Wiggins, P. P. Singh, and P. T. Debevic, Phys. Rev. C **26**, 2424 (1982).
[28]H. Machner, D. Protic, G. Riepe, J. P. Didelez, N. Frascaria, E. Gerlic, E. Hourani, and M. Morlet, Phys. Lett. **138B**, 39 (1984).
[29]J. W. Wachter, W. A. Gibson, and W. R. Burrus, Phys. Rev. C **6**, 1496 (1972).
[30]S. M. Beck and C. A. Powell, N. A. S. A. technical note NASA TN D-8119, 1976.
[31]K. R. Cordell, S. T. Thornton, L. C. Dennis, R. R. Doering, R. L. Parks, and T. C. Schweizer, Nucl. Phys. **A352**, 485 (1981).
[32]J. Bisplinghoff, J. Ernst, R. Lohr, T. Mayer-Kuckuk, and P. Meyer, Nucl. Phys. **A269**, 147 (1976).
[33]R. W. West, Phys. Rev. **141**, 1033 (1966).
[34]F. E. Bertrand, R. W. Peelle, and C. Kalbach-Cline, Phys. Rev. C **10**, 1028 (1974).
[35]H. Machner, G. Seniwongse, P. Jahn, M. Nolte, M. Rogge, and P. Turek, Phys. Rev. C **33**, 1931 (1986).
[36]B. Ludewigt, R. Glasow, H. Löhner, and R. Santo, Nucl. Phys. **A408**, 359 (1983).
[37]J. R. Wu, C. C. Chang, and H. D. Holmgren, Phys. Rev. C **19**, 659 (1979).
[38]K. R. Cordell, S. T. Thornton, L. C. Dennis, R. R. Doering, R. L. Parks, and T. C. Schweizer, Nucl. Phys. **A362**, 431 (1981).
[39]H. Machner, V. Bechstedt, A. Djaloeis, and P. Jahn, Phys. Rev. C **26**, 411 (1982).

[40]C. Kalbach, Z. Phys. A **283**, 401 (1977).
[41]F. E. Bertrand, W. R. Burrus, N. W. Hill, T. A. Love, and R. W. Peelle, Nucl. Instrum. Methods **101**, 475 (1972).
[42]A. A. Cowley, C. C. Chang, and H. D. Holmgren, Phys. Rev. C **22**, 2633 (1980).
[43]W. D. Myers and W. J. Swiatecki, Nucl. Phys. **81**, 1 (1966).
[44]J. R. Wu, C. C. Chang, and H. D. Holmgren, Phys. Rev. Lett. **40**, 1013 (1978).
[45]J. R. Wu, C. C. Chang, H. D. Holmgren, and R. W. Koontz, Phys. Rev. C **20**, 1284 (1979).
[46]A. Budzanowski, G. Baur, R. Shyam, J. Bojowald, W. Oelert, G. Riepe, M. Rogge, P. Turek, F. Rösel, and D. Trautman, Z. Phys. A **293**, 293 (1979).
[47]G. Baur, R. Shyam, F. Rösel, and D. Trautman, Phys. Rev. C **21**, 2668 (1980).
[48]T. Udagawa, X.-H. Li, and T. Tamura, Phys. Lett. **135B**, 333 (1984); **143B**, 15 (1984).
[49]J. R. Wu, C. C. Chang, and H. D. Holmgren, Phys. Rev. C **19**, 370 (1979).